# Mechanism of the Fe-Assisted Hydrothermal Liquefaction of Lignocellulosic Biomass

Miyata, Yoshinori ; Sagata, Kunimasa ; Yamazaki, Yoshiko ; Teramura, Hiroshi ; Hirano, Yoshiaki ; Ogino, Chiaki ; Kita, Yuichi

(Citation)
Industrial & Engineering Chemistry Research,57(44):14870-14877

(Issue Date)
2018-11-07

(Resource Type)
journal article

(Version)
Accepted Manuscript

# Mechanism of the Fe-Assisted Hydrothermal Liquefaction of Lignocellulosic Biomass

*Yoshinori Miyata,*[a,b] *Kunimasa Sagata,*[b] *Yoshiko Yamazaki,*[b] *Hiroshi Teramura,*[c] *Yoshiaki Hirano,*[b*] *Chiaki Ogino,*[b] *and Yuichi Kita*[b]

[a] New Business Planning Department, Nippon Shokubai Co., Ltd., Suita, Osaka 564-8512, Japan

[b] Department of Chemical Science and Engineering, Graduate School of Engineering, Kobe University, Kobe 657-8501, Japan

[c] Graduate School of Science, Technology and Innovation, Kobe University, Kobe 657-8501, Japan

**ABSTRACT**

Hydrothermal liquefaction (HTL) is a promising technique for converting biomass feedstocks to fuel and fine chemicals. A metallic Fe additive increases the water-soluble (WS) products of HTL, although the mechanism is unclear. Herein, commercially available carbohydrates (poly- and monosaccharides) and lignin isolated by enzymatic saccharification of palm empty fruit bunch were used as model substrates in the evaluation of the effect of Fe on HTL product composition. For carbohydrates, Fe and oxidized Fe synergistically contributed to the production of light compounds in the WS fraction by accelerating the retro-aldol condensation of sugars and suppressing the recondensation of unstable intermediates. The reactive intermediates could be stabilized by an electron-transfer-type reduction. On the other hand, Fe showed minimal effect on the HTL of enzymatic lignin, which was mainly converted to water-insoluble products. The results for the model substrates provided a picture of the overall pathway of Fe-assisted HTL of biomass.

## 1. INTRODUCTION

Reduction of greenhouse gas emissions to mitigate climate change is an urgent global issue given the ever-increasing worldwide energy consumption. An effective means to achieve a sustainable society is switching the source of chemical feedstocks from fossil fuels to carbon-neutral resources. Since biomass is one of the most abundant renewable resources, various biological and thermochemical methods have been developed to convert it into the easily manageable liquid form. Hydrothermal liquefaction (HTL) is a promising technology because it simply uses water as the solvent and directly converts biomass without any energy-consuming pre-drying step.[1-3] In HTL, biomass is treated with hot compressed water to afford water-soluble (WS) and water-insoluble (WI) fractions as main products and the gaseous fraction and solid residue (SR) as byproducts.[4]

While the WI fraction (so-called biocrude) has been investigated because of its utilization as a feedstock for liquid fuel, the WS fraction has attracted attention because its effective use is the key to making the whole process commercially feasible.[5] One of several methods of utilizing the WS fraction is recirculation into HTL itself, which enables the greater recovery of the oil yield and reduction of the loss of organics.[6-8] Anaerobic digestion to produce methane, which will maximize energy production, has also been proposed.[9] Gasification is a viable option to obtaining hydrogen for the biocrude upgrading process.[10] Organic acids in the WS fraction can be converted to ketones,[11] and subsequently, to liquid fuels or olefins through catalytic processes.[5] In addition, high-value specialty chemicals, such as ethanol, acetic acid, and acetone, can be produced by extraction and subsequent catalytic processes.[12]

Recently, we developed an HTL process for lignocellulosic biomass conversion using metallic Fe as an

additive. Oil palm empty fruit bunch (EFB) was efficiently liquefied to afford an especially large amount of WS fraction.[13] We focused on the WS fraction because it is a promising source of renewable chemical feedstocks; its aggressive utilization by catalytic cracking using a solid acid catalyst (HZSM-5 zeolite) produces hydrocarbons, such as olefinic and aromatic compounds.[14] The WS fraction produced through Fe-assisted HTL exhibited higher hydrocarbon yields than conventional HTL. The hydrocarbon yield of catalytic cracking is known to depend on the elemental composition of the feedstock.[15] Qualitative and quantitative analyses revealed that the Fe additive improved the elemental composition (i.e., increased H/C and decreased O/C ratios) in the WS fraction. In addition, Fe significantly increased the yield of light compounds. The WS fraction was successfully separated into a volatile fraction (light WS), containing mainly small compounds, and a non-volatile fraction (heavy WS), containing mainly oligomeric compounds. Catalytic cracking of light WS afforded more hydrocarbons than that of heavy WS, indicating that the degree of degradation in HTL is an important factor in the economics of the integrated process (HTL + cracking).[16]

The main components of biomass — cellulose, hemicellulose, and lignin — are decomposed under hydrothermal condition to form various products. Because of the complexity of the biomass composition, the reaction chemistry and mechanism of HTL are also complicated. The main pathway of HTL is believed to involve three steps: (i) depolymerization of biomass, (ii) decomposition of biomass monomers, and (iii) recondensation of reactive intermediates.[3] On the basis of the reactivity of saccharides and a few possible intermediates in Fe-assisted HTL, we hypothesized that step (ii) is accelerated, while step (iii) is

suppressed in the Fe/$H_2O$ system.[13] However, our previous study was limited to the effect of Fe on the reactivity of carbohydrate substrates and their decomposition products. The effect on lignin reactivity was not evaluated and the detailed role of Fe in the hydrothermal system remains unclear. These unresolved issues are obstacles to the optimization of the HTL process conditions.

In the present study, we further investigated the Fe-assisted HTL of biomass by evaluating the reactivity of each biomass component in the presence of Fe. Commercially available carbohydrates (including polysaccharides and monomeric sugars) and enzymatically isolated lignin were used as model substrates. Experiments were conducted in the presence and absence of Fe to elucidate the role of Fe and reaction mechanism in the Fe/$H_2O$ system. The contribution of each component of EFB to the products of Fe-assisted HTL was discussed on the basis of the results of the HTL of these model substrates.

## 2. EXPERIMENTAL SECTION

### 2.1 Materials

EFB from Indonesia was used as the lignocellulosic biomass feedstock and supplied by Nippon Shokubai Co., Ltd. It was dried at 25 ℃ and crushed into particles less than 300 μm in size. Fe powder (99.9%, NM-0029-UP) and $Fe_3O_4$ (98%, NO-0049-HP) were purchased from Ionic Liquids Technologies GmbH. Cellulose (Avicel® PH-101), alkali lignin, Celluclast® 1.5 L, and Novozyme 188 were purchased from Sigma-Aldrich Co., LLC. D-(+)-glucose and xylan from corn core were purchased from Wako Pure Chemical Industries, Ltd. and Tokyo Chemical Industry Co., Ltd., respectively.

### 2.2 HTL Process

HTL and separation experiments were performed according to a previously published method.[13] Briefly, the substrate, Fe powder, and deionized water were introduced into the Hastelloy C high-pressure reactor (MMJ-100, OM Labotech), which was purged four times with nitrogen after introduction of the materials. The initial pressure was set to 1.0 MPa with nitrogen, and the stirring rate was adjusted to 700 rpm. The reactor was then heated to the desired temperature. After a specific reaction time, the reactor was rapidly cooled to 25 °C using ice-water.

Gaseous products were collected in a gas sampling bag, and water-soluble products were isolated by filtration and denoted as the "WS" fraction. The water-insoluble solids in the filter cake were extracted with acetone and concentrated under reduced pressure as the "WI" fraction. The residue from the filter paper was dried and designated as "SR."

The WS fraction was freeze-dried using a modified method from our previous work.[16] The crude WS fraction (10 mL) was placed in a round-bottom flask and frozen by immersing the flask in liquid nitrogen. Immediately after connecting the flask to a freeze dryer (FDS-1000, Tokyo Rikakikai Co., Ltd.), the sample was maintained under reduced pressure (< 0.2 kPa) for 6 h. The volatile fraction was removed as "light WS" fraction, whereas the residue in the flask was collected by redissolution in water and denoted as "heavy WS" fraction.

**2.3 Analysis of HTL Products**

Gaseous products were analyzed using the Shimadzu GC-8A chromatograph equipped with silica-gel and 5A-molecular-sieve columns (ZS-74 and ZM-1, respectively, Shinwa Chemical Industries), and a thermal

conductivity detector. The total organic carbon (TOC) contents of the crude and heavy WS fractions were measured using a TOC analyzer (TOC-LCSH/CSN, Shimadzu). The TOC of the light WS fraction was the difference between those of the crude and heavy WS fractions. Identification of each product in the WS fraction was performed by gas chromatography-mass spectrometry (GC-MS) on the Shimadzu QP-2010 system equipped with a capillary column (Inert-cap® WAX-HT, 30 m × 0.25 mm ID × 0.25 μm film thickness, GL Sciences), while quantification was performed by gas chromatography-flame ionization detection (GC-FID) on the Shimadzu GC-2014 system equipped with the same capillary column. The WS fraction samples were diluted with acetone (1:1 v/v), and 2-methoxyethanol (0.05 wt%) was added as an internal standard. Compounds were identified by comparing their mass spectra to those from the National Institute of Standards and Technology library of mass spectral data. Elemental analysis (CHN) of WI and SR was performed using an elemental analyzer (vario EL cube, Elementar) and sulfanilamide as the calibration standard. The oxygen mass content was calculated from the difference.

The product yields from HTL were calculated as follows:

$$\text{Yield of each product from HTL (\%)} = \frac{\text{Moles of carbon in the product}}{\text{Moles of carbon in the raw material}} \times 100 \quad (1)$$

**2.4 Enzymatic Lignin Preparation**

Lignin was isolated by removal of cellulose and hemicellulose through ball-milling pretreatment and subsequent enzymatic saccharification.[17] EFB was introduced into a ball-mill (Simoloyer CM01, Zoz GmbH) and crushed at 1000 rpm for 120 min using 5-mm stainless steel beads. The vessel was kept at 5 °C during milling. Enzymatic saccharification was performed using an enzyme cocktail consisting of

Celluclast® 1.5 L (280 Units/g EFB) and Novozyme 188 (10 Units/g EFB). The crushed EFB (30 g), enzyme cocktail, and 0.1 M sodium acetate buffer (pH 5.0, 260 g) were placed in a plastic container with a lid and then, the reaction mixture was incubated at 50 °C for 21 h with agitation using a shaker. The solid content was collected from the resulting slurry by centrifugation and washed with deionized water. Saccharification was repeatedly performed on the solid residue, and wet enzymatic lignin was obtained in 27 wt% yield as a solid.

**2.5 Analysis of Carbohydrates and Total Lignin**

The compositions of raw EFB and enzymatic lignin were determined using the analytical procedure reported by the National Renewable Energy Laboratory (NREL).[18] Quantification of carbohydrates (cellulose and hemicellulose) and acetic acid was performed by high-performance liquid chromatography (Prominence, Shimadzu) equipped with Aminex® HPX-87H columns (300 mm × 7.8 mm ID, Bio-Rad) and a refractive index detector. The acid-soluble lignin was determined using a UV-visible spectrophotometer (UVmini-1240, Shimadzu), and the acid-insoluble lignin was defined as the ash-free solid residue (Klason lignin).

**3. RESULTS AND DISCUSSION**

**3.1 Hydrothermal Liquefaction of Carbohydrates**

*3.1.1 Effect of Metallic Fe*

To investigate the effect of Fe on the HTL of carbohydrates, various carbohydrates including mono- and polysaccharides were reacted under hydrothermal condition (10 wt% raw material, 300 °C, 10 min) both in

the presence and absence of Fe. The results are compared to that for EFB, as shown in Figure 1. Products were collected as four fractions: WS, WI, gaseous products, and SR. In all cases, the addition of Fe significantly increases the yield of WS, and lowers those of WI and SR. As we reported in a previous paper, Fe-assisted HTL of carbohydrates afforded significant amounts of alcohols (hydroxyketones such as hydroxyacetone), which contributed to a higher WS fraction. Retro-aldol condensation of sugars was considered to be promoted by the oxidized Fe generated in situ, and subsequent hydrogenation of the resulting aldehydes afforded alcohols.[13] There is only minor difference between the HTL of cellulose and glucose both in the presence and absence of Fe. This implies that Fe has an insignificant effect on the depolymerization of cellulose to glucose by hydrolysis since this process is known to occur rapidly under hydrothermal condition.[19] The C5 sugar (xylan) exhibits lower WS yield and higher WI yield in the presence of Fe than the C6 sugar. Nevertheless, both C5 and C6 sugars show increased WS yield and suppressed char production after the addition of Fe. These results confirm that Fe is effective for the conversion of the carbohydrate components of biomass feedstocks into the WS fraction. In contrast, Fe has less effect on lignin; compared with carbohydrates, HTL of EFB results in lower WS yield and higher WI yield both in the presence and absence of Fe. Therefore, the lignin in EFB is more likely to be converted to WI rather than WS under hydrothermal condition. This is supported by the fact that the WS fraction produced from HTL of EFB contained only small amounts of phenolic products[16] produced by depolymerization of lignin.[3] At least Fe is not considered to have the ability to decompose lignin into monomeric units.

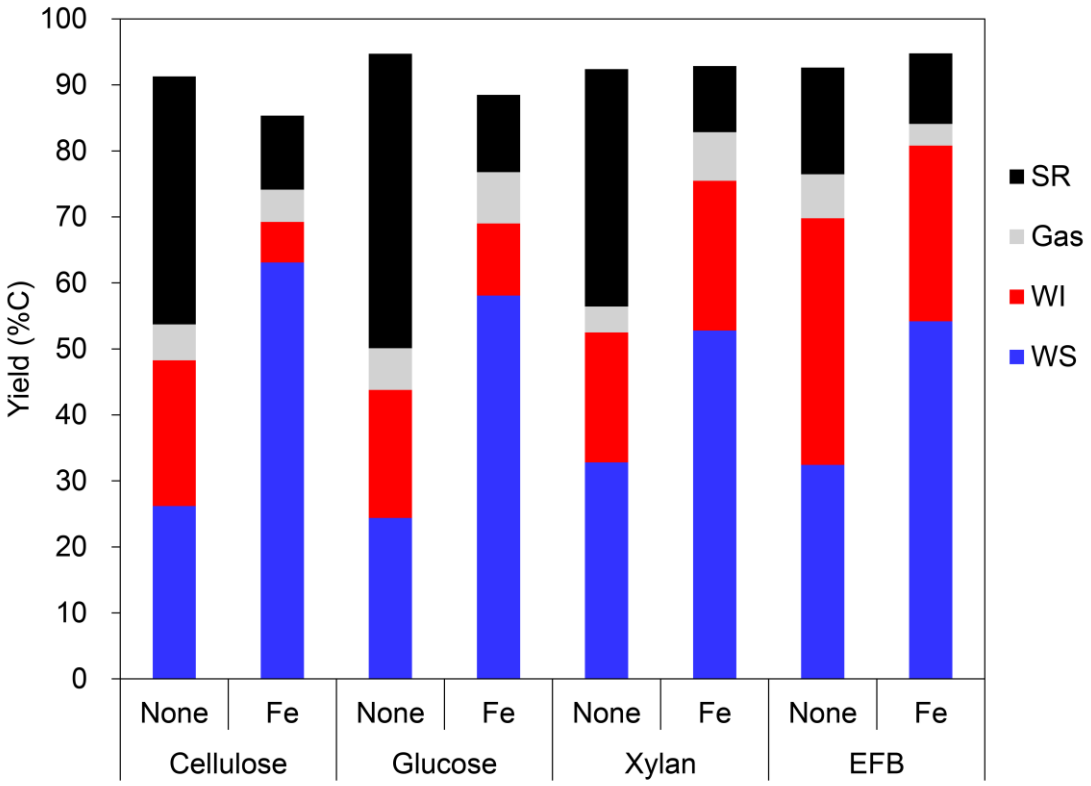


**Figure 1.** Product yields of HTL of carbohydrates and EFB in the presence and absence of Fe.

*3.1.2 Effect of Oxidized Fe*

A number of studies on the effect of various catalysts in HTL have been reported.[20-23] Bases (e.g., $K_2CO_3$, KOH) are representative catalysts that promote the hydrolysis of glycosidic linkages and facilitate the endwise depolymerization of carbohydrates.[20] Fe compounds (e.g., $FeCl_3$, $Fe_2O_3$, $FeSO_4$) also act as catalysts in HTL, which increase the yield of biocrude (WI fraction) while suppressing the formation of char (SR).[23] We have previously demonstrated the transformation of glucose to C3 chemicals in water using oxidized metals or metallic Fe.[24, 25] In these works, we considered the oxidized Fe species as a retro-aldol catalyst.[26-28] To investigate the role of oxidized Fe, HTL of glucose using Fe and/or $Fe_3O_4$ was

performed (Figure 2). When $Fe_3O_4$ is the only additive, the WS yield is higher than that of normal HTL; however, its effect is smaller than that of Fe even though the same amount of additive (based on Fe) is used. The WI yield increases, while SR production is suppressed, compared with product yields obtained without catalyst loading, which is consistent with the results of other HTL using an oxidized Fe catalyst.[23] However, higher WS yield and lower WI yield are obtained using both additives compared with using Fe alone, indicating the synergistic effect of Fe and $Fe_3O_4$. We determined the ratio of the volatile and non-volatile fractions in WS (indicated as light and heavy WS in Figure 2, respectively) using the freeze-dry method. In addition, GC analysis of the WS fraction and quantification of the products were conducted using previously reported methods (Figure 3, Table S1).[16] Although a smaller quantity of volatile compounds is detected using $Fe_3O_4$ compared with using Fe, the WS profile using $Fe_3O_4$ was different from that using conventional HTL. For example, 4-oxo-pentanoic acid, which is produced by dehydration of glucose, was not detected in the $Fe_3O_4$ system. On the other hand, small amounts of C2-C4 products were detected. The combination of Fe and $Fe_3O_4$ was also found to maximize the yield of small molecules. These results indicate that the catalytic activity of oxidized Fe alone is relatively low and only efficiently increases the amount of volatile WS products by coexisting with metallic Fe in the system. Since only Fe is used as an additive in the present system, the concentration of oxidized Fe and consequently, the retro-aldol activity, were initially low. The WS yield can be improved by using oxidized Fe (i.e., incompletely reduced Fe) or other retro-aldol catalysts as co-additive.

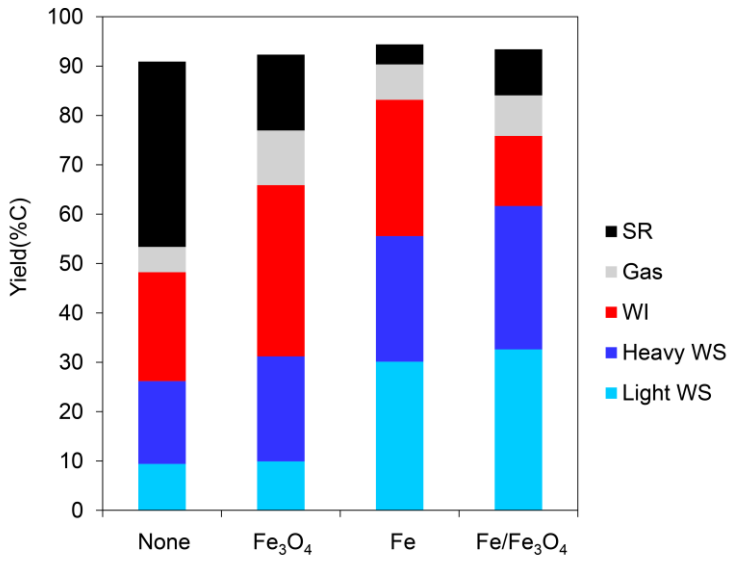


**Figure 2.** Product profile of HTL of glucose in the absence and presence of various additives.

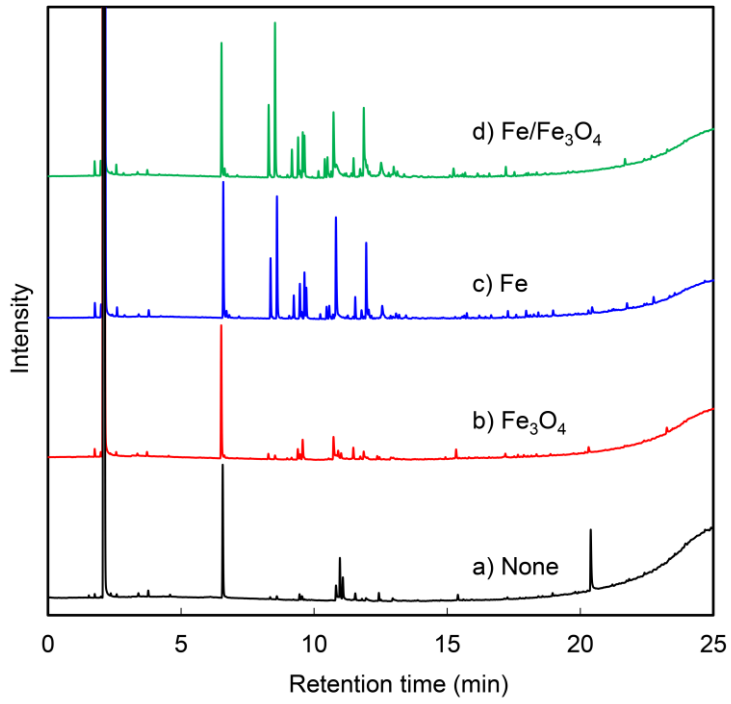


**Figure 3.** GC-FID chromatograms of the WS fraction from HTL of glucose (a) without additive and in the presence of (b) $Fe_3O_4$, (c) Fe, and (d) $Fe/Fe_3O_4$.

*3.1.3 Hydrogenation by Metallic Fe*

As shown in Section 3.1.2, efficient decomposition of sugars is achieved by the combined effects of oxidized and metallic Fe. Unstable carbonyl compounds, especially aldehydes, produced via retro-aldol condensation of sugars can easily undergo recondensation to form insoluble polymers (WI) and char (SR). Fe is considered to reduce these labile intermediates to stable alcohols, which suppresses the formation of byproducts. In our previous work, we confirmed that pyruvaldehyde could be hydrogenated under hydrothermal condition in the presence of Fe to produce hydroxyacetone.[13] According to the literature,[29-31] there are a few possible hydrogenation pathways using zero-valent metal in water (Scheme 1). Pathway (i) is initiated by the attack of a highly active hydrogen radical, generated from metallic Fe and a proton, on the carbonyl group. Pathway (ii) is initiated by hydride transfer from an iron hydride species generated from metallic Fe and a proton. Pathway (iii) involves single-electron transfer from metallic Fe to the substrate as the key step. The hydrogen radical in pathway (i) was originally assigned as the so-called "nascent hydrogen"; however, its existence was rejected by several succeeding studies.[29, 30] Fábos et al. proposed pathway (ii) as an alternate explanation for the "nascent hydrogen" in their work on the mechanism of hydrogenation using metallic Fe and acids.[31] The most general explanation for hydrogenation reactions using zero-valent metals is pathway (iii), which is analogous to the Bouveault-Blanc reduction in which esters are converted into alcohols by metallic Na.[32, 33] Reduction of aldehydes had also been achieved using Fe, Zn, Mg, Al and Mn as a reductant.[34-38] Mechanism has been proposed in which aldehydes adsorbed on the surface of Fe are reduced by single electron transfer from Fe

to form radical intermediates.[36] In addition, we found that the reaction of benzaldehyde in this hydrothermal reduction system affords benzyl alcohol and diphenyl acetaldehyde as byproduct (Scheme S1). The latter is considered to form through pinacol-type homocoupling of radical intermediates[35, 38, 39] and subsequent pinacol rearrangement,[40] which is circumstantial evidence for the generation of radical intermediates. According to these considerations, we conclude that pathway (iii) is the most plausible route for the present reaction system. It should be noted that $H_2$ does not participate in hydrogenation in any of the three pathways despite being present in the gas phase of Fe-assisted HTL of biomass due to the direct reaction of Fe and water ($3Fe + 4H_2O \rightarrow Fe_3O_4 + 4H_2$). We estimate that in HTL of EFB, about half of the reducing capacity of Fe was used for the reduction of the products, while the remaining half was used for the reaction with water (Tables S2-S4). To efficiently utilize the reducing capacity of Fe, other hydrogenation catalysts are required.

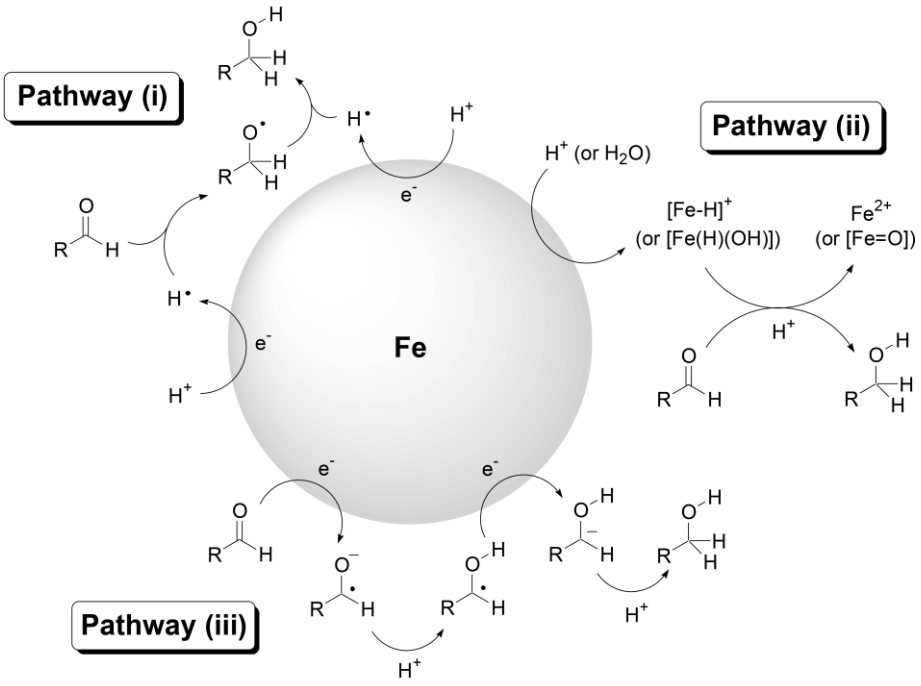


**Scheme 1. Possible pathways of hydrogenation by metallic Fe under hydrothermal condition**

### 3.2 Effect of Fe on HTL of Lignin

*3.2.1 Preparation of Enzymatic Lignin*

To evaluate the reactivity of lignin in HTL of lignocellulosic biomass and the effect of Fe, it is crucial to examine the reaction of pure lignin. However, there are no known methods to isolate lignin in its natural form. Commercially available lignins (e.g., alkali lignin, lignosulfonic acid) have undergone strong alkali and high-temperature treatments. Under these harsh conditions, deconstruction of ether bonds (β-O-4 bond cleavage) and condensation (C–C bond formation) simultaneously occur,[41] making these substrates unsuitable for accurate evaluation of HTL of lignin. Therefore, we chose enzymatic lignin as the model substrate for HTL. It is prepared by ball-milling of raw biomass and subsequent enzymatic hydrolysis of carbohydrates. The lignin produced by this process is known to have a structure relatively close to that of natural lignin and is sometimes used as model substrate for lignin depolymerization.[42, 43] The composition of the prepared enzymatic lignin was determined using the NREL method[18] and is summarized in Figure 4. The amount of lignin is the sum of acid-soluble and acid-insoluble fractions. Compared with the raw material before enzymatic hydrolysis, enzymatic lignin has a significantly reduced proportion of C6 and C5 carbohydrates, although its lignin content increases from 27% to 61% by weight.

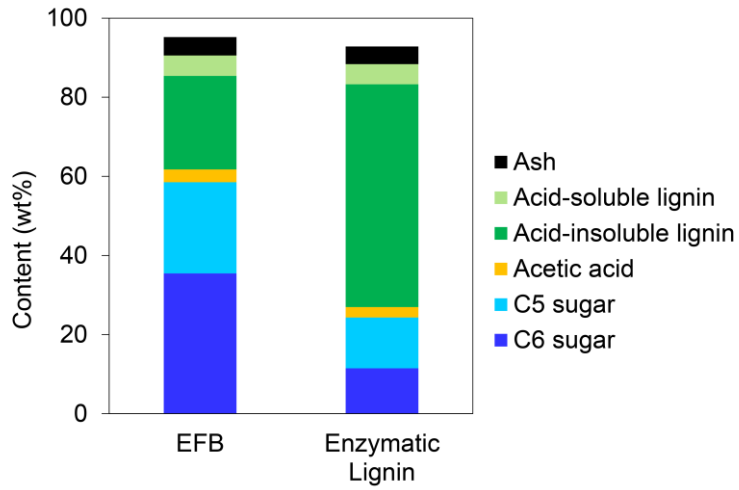


**Figure 4.** Compositions of EFB and enzymatic lignin determined using the NREL method.

*3.2.2 Effect of Lignin Concentration on HTL*

The reactivity of lignin in HTL in the presence and absence of Fe was estimated by testing various substrates with different lignin contents: (A) a mixture of cellulose and xylan (6:4 by weight, the same proportion in EFB, 0% lignin), (B) EFB (27% lignin), and (C) enzymatic lignin (61% lignin). In addition, (D) alkali lignin (100% lignin) was used as the reference sample. The product yields are summarized in Table S5, and plots of each product yield versus lignin content are shown in Figure 5. The yields using the mixture of cellulose and xylan (A) are similar to those using cellulose or xylan alone. There are significant differences between the WS and WI yields of Fe-assisted and conventional HTL. On the other hand, for lignin-containing substrates (B and C), the WS yield decreases linearly, while the WI yield increases linearly, with lignin content, and the difference between the product yields of Fe-assisted and conventional HTL is smaller. In the presence of Fe, enzymatic lignin affords only 9% higher WS fraction and 5% lower WI fraction compared with the product yields obtained in conventional HTL. When each yield is

extrapolated to 100% lignin content, there is only minor difference between Fe-assisted and conventional HTL. The reaction of alkali lignin (D) results in low WS yield as well as high WI yield, which are close to the extrapolated values (Table S5). In all cases, small amounts of phenolic compounds, which are the products of lignin depolymerization, were observed in WI by GC analysis. These results indicate that lignin is easily converted to the WI fraction through the HTL process owing to their high molecular weight and hydrophobicity, and Fe is not effective for depolymerizing lignin to small compounds. In addition, the elemental compositions of WI from Fe-assisted and conventional HTL, determined by CHN analysis, were almost the same, showing that hydrodeoxygenation of lignin did not proceed after the addition of Fe. Based on the aforementioned results, Fe as an additive is considered to exhibit insignificant effect on the HTL of lignin in biomass feedstocks.

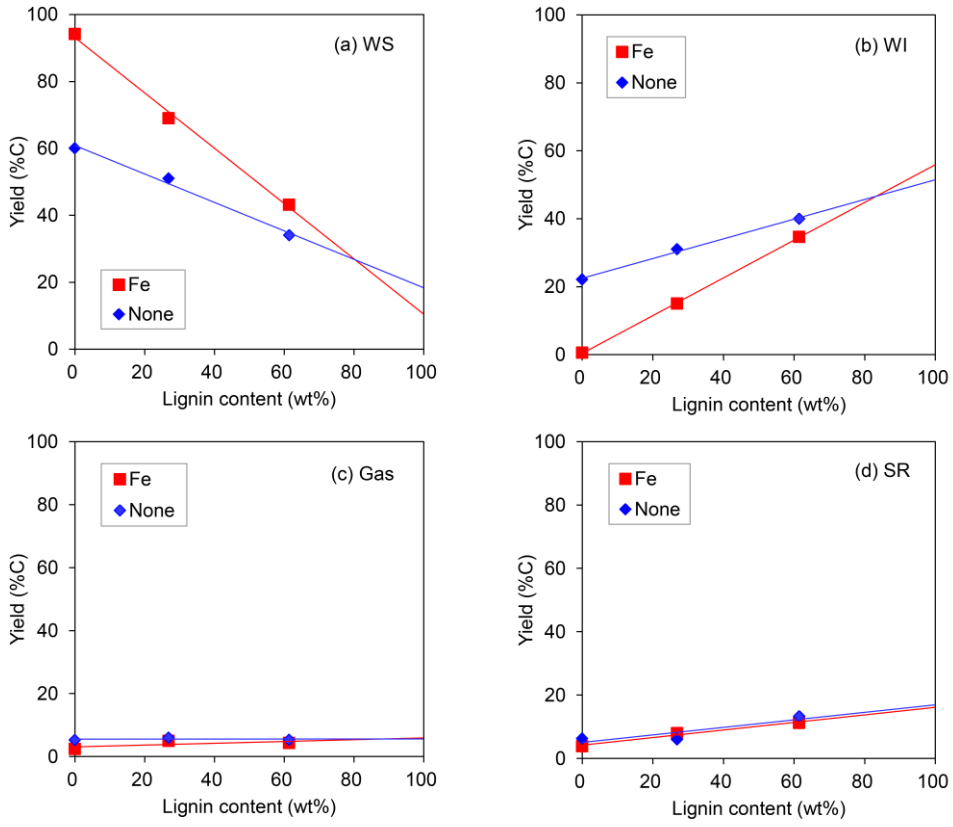

**Figure 5.** Product yields from HTL at various lignin contents of model substrates: 0% (6:4 mixture of cellulose/xylan), 27% (EFB), and 61% (enzymatic lignin). (a) WS, (b) WI, (c) Gas, and (d) SR fractions.

### 3.3 Contribution of Each Component of EFB to Fe-Assisted HTL Yields

After evaluating the reactivity of all components of the biomass, we estimated the material balance of Fe-assisted HTL. The composition of 4 g of EFB determined using the NREL method is shown in Table 1. The yields of Fe-assisted HTL of individual components at quantities close to their concentrations in EFB are summarized in Table 2. Using the data in Tables 1 and 2, the contributions of each component to each fraction were calculated and summed to obtain the estimated yield of Fe-assisted HTL of EFB (Table 3). These estimated values are close to the actual performance of Fe-assisted HTL of EFB (Figure 6). Therefore, the Fe-assisted reaction of EFB can be approximated by summing the reaction of individual components. Table 3 reveals the breakdown of the products from each component, showing that cellulose and xylan mainly contribute to the WS yield, whereas the amount of WS products derived from lignin is small.

**Table 1. Composition of EFB (4 g)[a]**

| | Content (wt%) | Weight (g) |
|---|---|---|
| Cellulose | 39 | 1.4 |
| Xylan | 23 | 0.9 |
| Lignin[b] | 29 | 1.2 |
| Total | 87 | 3.4 |

[a]Determined using NREL method. [b]Sum of acid-soluble and acid-insoluble lignin.

**Table 2. HTL of model substrates in the presence of Fe [a]**

| | Substrate | Product Yields (%C/Substrate) | | | | Carbon Balance |
|---|---|---|---|---|---|---|
| | (g) | WS | WI | Gas | SR | (%C) |
| Cellulose | 1.5 | 77 | 2 | 6 | 4 | 89 |
| Xylan | 1 | 80 | 4 | 7 | 3 | 94 |
| Lignin[b] | 1 | 11 | 56 | 6 | 16 | 89 |

[a]Reaction conditions: $H_2O$ = 40 g, Fe = 1.564 g/substrate, atmosphere = 1.0 MPa ($N_2$), temperature = 300 °C, time = 10 min. Yields were calculated as carbon yield based on the starting materials. [b]Yields were estimated from Figure 5 by extrapolating to 100% lignin content.

**Table 3. Estimated contributions to the yield of EFB liquefaction (%C) [a]**

| | Contribution (%C/EFB) | | | | Carbon balance |
|---|---|---|---|---|---|
| | WS | WI | Gas | SR | (%C) |
| Cellulose | 26 | 1 | 2 | 1 | 30 |
| Xylan | 18 | 1 | 1 | 1 | 21 |
| Lignin | 4 | 22 | 2 | 6 | 34 |
| Total | 48 | 24 | 5 | 8 | 85 |

[a]Contribution of each component was calculated by multiplying the carbon content of the component in EFB by its HTL yield.

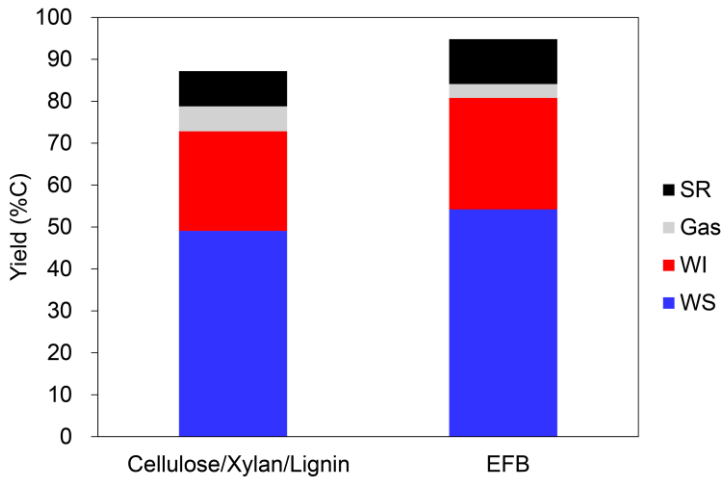


**Figure 6.** Yields estimated from HTL of each model substrate (cellulose, xylan, and lignin) (left) and obtained from HTL of EFB (right).

### 3.4 Proposed Overall Reaction Pathway

On the basis of reaction routes investigated herein and our previous work,[13, 16] we propose the overall reaction pathway shown in Scheme 2. Polysaccharides (cellulose and hemicellulose) are rapidly hydrolyzed under hydrothermal condition to C6 and C5 sugars. These sugars isomerize between their aldose and ketose forms and are cleaved through retro-aldol condensation catalyzed by oxidized Fe. The resulting C2-C4 intermediates easily undergo isomerization (keto-enol tautomerization), dehydration/hydration, or recondensation owing to the presence of the carbonyl group, which makes the reaction system more complex. Recondensation increases the fractions of insoluble polymers (WI) and char (SR). However, hydrogenation in the presence of zero-valent Fe converts unstable aldehydes to alcohols, which are stable under hydrothermal condition and consequently increases the WS fraction. In

contrast, lignin is hardly depolymerized in the present Fe-assisted system and therefore recovered largely as the WI fraction.

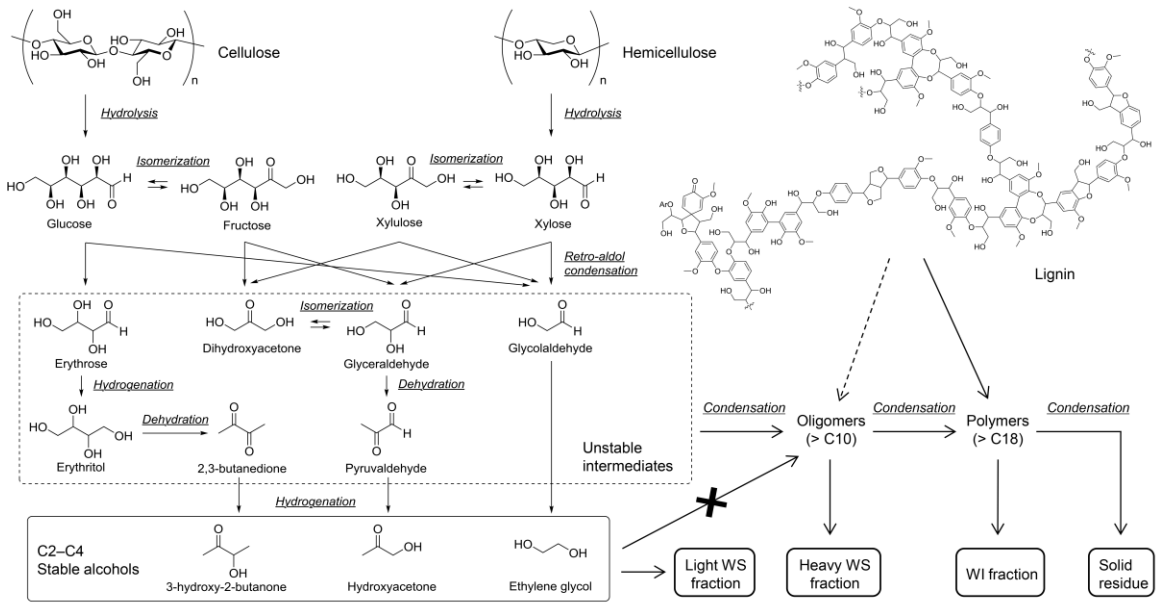


**Scheme 2. Plausible overall reaction pathway of Fe-assisted HTL of lignocellulosic biomass**

## 4. CONCLUSIONS

Metallic Fe and oxidized Fe generated in situ worked synergistically in HTL of biomass to increase the quantity of light compounds in the WS fraction. Oxidized Fe accelerated retro-aldol condensation of sugars, while Fe suppressed the recondensation of unstable intermediates. The Fe additive had minor effect on the degradation of enzymatic lignin. The material balance of Fe-assisted HTL of biomass was estimated from the reactions of individual model substrates. This HTL system can efficiently convert polysaccharides (e.g., cellulose and hemicellulose) to small compounds that can be used as feedstocks for production of specialty chemicals. Identification of reaction mechanisms will aid in the optimization of reaction conditions and

development of a total reaction system.

ASSOCIATED CONTENT

**Supporting Information.** The Supporting Information is available free of charge on the ACS Publications website at DOI:

GC quantification of light WS fraction from hydrothermal liquefaction of glucose, hydrothermal reaction of benzaldehyde, elemental balance of Fe-assisted hydrothermal liquefaction, and hydrothermal liquefaction of lignin model substrates (PDF)

AUTHOR INFORMATION

**Corresponding Author**

*E-mail: hirano@phoenix.kobe-u.ac.jp

**Notes**

The authors declare no competing financial interest.

**ACKNOWLEDGMENTS**

The authors gratefully acknowledge financial support from Nippon Shokubai Co., Ltd.

**REFERENCES**

(1) Gollakota, A. R. K.; Kishore, N.; Gu, S. A Review on Hydrothermal Liquefaction of Biomass. *Renewable Sustainable Energy Rev.* **2018**, *81*, 1378–1392.

(2) Kumar, M.; Olajire Oyedun, A.; Kumar, A. A Review on the Current Status of Various

Hydrothermal Technologies on Biomass Feedstock. *Renewable Sustainable Energy Rev.* **2018**, *81*, 1742–1770.

(3) Toor, S. S.; Rosendahl, L.; Rudolf, A. Hydrothermal Liquefaction of Biomass: A Review of Subcritical Water Technologies. *Energy* **2011**, *36*, 2328–2342.

(4) Sun, P.; Heng, M.; Sun, S.-H.; Chen, J. Analysis of Liquid and Solid Products from Liquefaction of Paulownia in Hot-Compressed Water. *Energy Convers. Manage.* **2011**, *52*, 924–933.

(5) Madsen, R. B.; Biller, P.; Jensen, M. M.; Becker, J.; Iversen, B. B.; Glasius, M. Predicting the Chemical Composition of Aqueous Phase from Hydrothermal Liquefaction of Model Compounds and Biomasses. *Energy Fuels* **2016**, *30*, 10470–10483.

(6) Biller, P.; Madsen, R. B.; Klemmer, M.; Becker, J.; Iversen, B. B.; Glasius, M. Effect of Hydrothermal Liquefaction Aqueous Phase Recycling on Bio-Crude Yields and Composition. *Bioresour. Technol.* **2016**, *220*, 190–199.

(7) Klemmer, M.; Madsen, R. B.; Houlberg, K.; Mørup, A. J.; Christensen, P. S.; Becker, J.; Glasius, M.; Iversen, B. B. Effect of Aqueous Phase Recycling in Continuous Hydrothermal Liquefaction. *Ind. Eng. Chem. Res.* **2016**, *55*, 12317–12325.

(8) Ramos-Tercero, E. A.; Bertucco, A.; Brilman, D. W. F. Process Water Recycle in Hydrothermal Liquefaction of Microalgae to Enhance Bio-Oil Yield. *Energy Fuels* **2015**, *29*, 2422–2430.

(9) Tommaso, G.; Chen, W. T.; Li, P.; Schideman, L.; Zhang, Y. Chemical Characterization and Anaerobic Biodegradability of Hydrothermal Liquefaction Aqueous Products from Mixed-Culture

Wastewater Algae. *Bioresour. Technol.* **2015**, *178*, 139–46.

(10) Cherad, R.; Onwudili, J. A.; Biller, P.; Williams, P. T.; Ross, A. B. Hydrogen Production from the Catalytic Supercritical Water Gasification of Process Water Generated from Hydrothermal Liquefaction of Microalgae. *Fuel* **2016**, *166*, 24–28.

(11) Wu, K.; Yang, M.; Chen, Y.; Pu, W.; Hu, H.; Wu, Y. Aqueous-Phase Ketonization of Acetic Acid over Zr/Mn Mixed Oxides. *AIChE J.* **2017**, *63*, 2958–2967.

(12) Maddi, B.; Panisko, E.; Wietsma, T.; Lemmon, T.; Swita, M.; Albrecht, K.; Howe, D. Quantitative Characterization of Aqueous Byproducts from Hydrothermal Liquefaction of Municipal Wastes, Food Industry Wastes, and Biomass Grown on Waste. *ACS Sustainable Chem. Eng.* **2017**, *5*, 2205–2214.

(13) Miyata, Y.; Sagata, K.; Hirose, M.; Yamazaki, Y.; Nishimura, A.; Okuda, N.; Arita, Y.; Hirano, Y.; Kita, Y. Fe-Assisted Hydrothermal Liquefaction of Lignocellulosic Biomass for Producing High-Grade Bio-Oil. *ACS Sustainable Chem. Eng.* **2017**, *5*, 3562–3569.

(14) Vispute, T. P.; Zhang, H. Y.; Sanna, A.; Xiao, R.; Huber, G. W. Renewable Chemical Commodity Feedstocks from Integrated Catalytic Processing of Pyrolysis Oils. *Science* **2010**, *330*, 1222–1227.

(15) Zhang, H.; Cheng, Y.-T.; Vispute, T. P.; Xiao, R.; Huber, G. W. Catalytic Conversion of Biomass-Derived Feedstocks into Olefins and Aromatics with ZSM-5: The Hydrogen to Carbon Effective Ratio. *Energy Environ. Sci.* **2011**, *4*, 2297–2307.

(16) Miyata, Y.; Yamazaki, Y.; Hirano, Y.; Kita, Y. Quantitative Analysis of the Aqueous Fraction

from the Fe-Assisted Hydrothermal Liquefaction of Oil Palm Empty Fruit Bunches. *J. Anal. Appl. Pyrolysis* **2018**, *132*, 72–81.

(17) Zhang, Y.; Yang, L.; Wang, D.; Li, D. Structure Elucidation and Properties of Different Lignins Isolated from Acorn Shell of Quercus variabilis Bl. *Int. J. Biol. Macromol.* **2018**, *107*, 1193–1202.

(18) Sluiter, A.; Hames, B.; Ruiz, R.; Scarlata, C.; Sluiter, J.; Templeton, D.; Crocker, D. *Determination of Structural Carbohydrates and Lignin in Biomass, Laboratory Analytical Procedure (LAP)*; National Renewable Energy Laboratory: Golden, CO, August 2012.

(19) Ehara, K.; Saka, S. Decomposition Behavior of Cellulose in Supercritical Water, Subcritical Water, and Their Combined Treatments. *J. Wood Sci.* **2005**, *51*, 148–153.

(20) Singh, R.; Balagurumurthy, B.; Prakash, A.; Bhaskar, T. Catalytic Hydrothermal Liquefaction of Water Hyacinth. *Bioresour. Technol.* **2015**, *178*, 157–165.

(21) Nazari, L.; Yuan, Z.; Souzanchi, S.; Ray, M. B.; Xu, C. Hydrothermal Liquefaction of Woody Biomass in Hot-Compressed Water: Catalyst Screening and Comprehensive Characterization of Bio-Crude Oils. *Fuel* **2015**, *162*, 74–83.

(22) Xu, C.; Etcheverry, T. Hydro-Liquefaction of Woody Biomass in Sub- and Super-Critical Ethanol with Iron-Based Catalysts. *Fuel* **2008**, *87*, 335–345.

(23) Li, H.; Hurley, S.; Xu, C. Liquefactions of Peat in Supercritical Water with a Novel Iron Catalyst. *Fuel* **2011**, *90*, 412–420.

(24) Hirano, Y.; Sagata, K.; Kita, Y. Selective Transformation of Glucose into Propylene Glycol on

Ru/C Catalysts Combined with Zno under Low Hydrogen Pressures. *Appl. Catal., A* **2015**, *502*, 1–7.

(25) Hirano, Y.; Kasai, Y.; Sagata, K.; Kita, Y. Unique Approach for Transforming Glucose to C3 Platform Chemicals Using Metallic Iron and a Pd/C Catalyst in Water. *Bull. Chem. Soc. Jpn.* **2016**, *89*, 1026–1033.

(26) Baeza, A.; Guillena, G.; Ramón, D. J. Magnetite and Metal-Impregnated Magnetite Catalysts in Organic Synthesis: A Very Old Concept with New Promising Perspectives. *ChemCatChem* **2016**, *8*, 49–67.

(27) Ramón, D.; Cano, R.; Yus, M. Unmodified Nano-Powder Magnetite or Iron(III) Oxide Catalyze the Easy and Fast Synthesis of 4-Substituted-4*h*-Pyrans. *Synlett* **2011**, *2011*, 2017–2020.

(28) Watanabe, H.; Seto, J. The Catalysis of Maghemite and Hematite on the Aldol and the Retro-Aldol Condensation of Acetone. *Bull. Chem. Soc. Jpn.* **1991**, *64*, 2411–2415.

(29) Laborda, F.; Bolea, E.; Baranguan, M. T.; Castillo, J. R. Hydride Generation in Analytical Chemistry and Nascent Hydrogen: When Is It Going to Be Over? *Spectrochim. Acta, Part B* **2002**, *57*, 797–802.

(30) Meija, J.; D'Ulivo, A. Solution to Nascent Hydrogen Challenge. *Anal. Bioanal. Chem.* **2008**, *392*, 771–772.

(31) Fábos, V.; Yuen, A. K. L.; Masters, A. F.; Maschmeyer, T. Exploring the Myth of Nascent Hydrogen and its Implications for Biomass Conversions. *Chem. - Asian J.* **2012**, *7*, 2629–2637.

(32) Bouveault, L.; Blanc, G. Préparation Des Alcools Primaires Au Moyen Des Acides Correspondants. *Comptes rendus hebdomadaires des séances de l'Académie des sciences* **1903**, *136*, 1676–

1678.

(33) Bouveault, L.; Blanc, G. Transformation Des Acides Monobasiques Saturés Dans Les Alcools Primaires Correspondants. *Bull. Soc. Chim. Fr.* **1904**, *31*, 666–672.

(34) Clarke, H. T.; Dreger, E. E. N-Heptyl Alcohol. *Org. Synth.* **1926**, *6*, 52–53.

(35) Mandal, T.; Jana, S.; Dash, J. Zinc-Mediated Efficient and Selective Reduction of Carbonyl Compounds. *Eur. J. Org. Chem.* **2017**, *2017*, 4972-4983.

(36) Zhang, W.-C.; Li, C.-J. Magnesium-Mediated Carbon-Carbon Bond Formation in Aqueous Media: Barbier-Grignard Allylation and Pinacol Coupling of Aldehydes. *J. Org. Chem.* **1999**, *64*, 3230–3236.

(37) Wei-Bo, W.; Li-Lan, S.; Yao-Zeng, H., A Novel Reduction System — $SbCl_3$-Al/ or $SbCl_3$-Zn/DMF-$H_2O$ for Conversion of Aldehydes to Alcohols. *Tetrahedron Lett.* **1990**, *31*, 1185–1186.

(38) Jiménez, T.; Barea, E.; Oltra, J. E.; Cuerva, J. M.; Justicia, J., Mn(0)-Mediated Chemoselective Reduction of Aldehydes. Application to the Synthesis of α-Deuterioalcohols. *J. Org. Chem.* **2010**, *75*, 7022–7025.

(39) Li, C.-J. Organic Reactions in Aqueous Media with a Focus on Carbon-Carbon Bond Formations: A Decade Update. *Chem. Rev.* **2005**, *105*, 3095–3166.

(40) Amedio, J. C., Jr.; Bernard, P. J.; Fountain, M.; VanWagenen, G. A., Jr. Practical Preparation of 4,4-Diphenylcyclohexanol: A Key Intermediate in the Synthesis of Ms-325. *Synth. Commun.* **1998**, *28*, 3895–3906.

(41) Chakar, F. S.; Ragauskas, A. J. Review of Current and Future Softwood Kraft Lignin Process Chemistry. *Ind. Crops Prod.* **2004**, *20*, 131–141.

(42) Jääskeläinen, A. S.; Sun, Y.; Argyropoulos, D. S.; Tamminen, T.; Hortling, B. The Effect of Isolation Method on the Chemical Structure of Residual Lignin. *Wood Sci. Technol.* **2003**, *37*, 91–102.

(43) Shen, X.-J.; Wen, J.-L.; Huang, P.-L.; Zheng, K.; Wang, S.-F.; Liu, Q.-Y.; Charlton, A.; Sun, R.-C. Efficient and Product-Controlled Depolymerization of Lignin Oriented by Raney Ni Cooperated with $Cs_xH_{3-x}PW_{12}O_{40}$. *BioEnergy Res.* **2017**, *10*, 1155–1162.

**TOC Graphic**

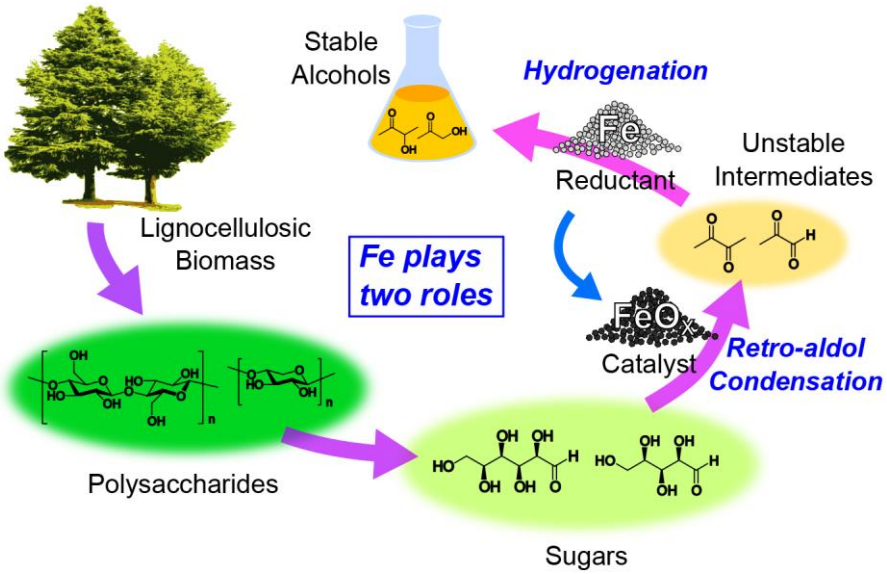
Stable
Alcohols
Hydrogenation
Fe
Reductant
Unstable
Intermediates
Lignocellulosic
Biomass
Fe plays
two roles
FeOx
Catalyst
Retro-aldol
Condondensation
Polysaccharides
Sugars

Supporting Information

# Mechanism of the Fe-Assisted Hydrothermal Liquefaction of Lignocellulosic Biomass

*Yoshinori Miyata,*[a,b] *Kunimasa Sagata,*[b] *Yoshiko Yamazaki,*[b] *Hiroshi Teramura,*[c] *Yoshiaki Hirano,*[b*] *Chiaki Ogino,*[b] *and Yuichi Kita*[b]

[a] New Business Planning Department, Nippon Shokubai Co., Ltd., Suita, Osaka 564-8512, Japan

[b] Department of Chemical Science and Engineering, Graduate School of Engineering, Kobe University, Kobe 657-8501, Japan

[c] Graduate School of Science, Technology and Innovation, Kobe University, Kobe 657-8501, Japan

* Corresponding author

Email address: hirano@phoenix.kobe-u.ac.jp (Yoshiaki Hirano)

Table of contents

**1. Gas chromatography quantification of light water-soluble fraction from hydrothermal liquefaction of glucose**

The volatile compounds in the water-soluble (WS) fraction, detected by gas chromatography (GC), were quantified using the relative response factor (RRF). RRF is defined by

$$\mathrm{RRF} = \frac{A_i \times C_{IS}}{C_i \times A_{IS}} \quad (1),$$

where *C* is the concentration, *A* is the peak area, and the subscripts *i* and *IS* refer to the analyte and internal standard, respectively.

The RRF of commercially available compounds were determined from experimental data. If the authentic sample was not available, the RRF was predicted following the previously reported method.[1]

**Table S1.** Quantitative analysis of WS fraction from hydrothermal liquefaction of glucose[a]

| Retention | | none | | $Fe_3O_4$[b] | | Fe[c] | | Fe + $Fe_3O_4$[d] | |
|---|---|---|---|---|---|---|---|---|---|
| time (min) | compound | Area | Yield (%C) | Area | Yield (%C) | Area | Yield (%C) | Area | Yield (%C) |
| 2.6 | 2-Butanone | 319 | 0.06 | 572 | 0.08 | 1668 | 0.23 | 1884 | 0.25 |
| 2.9 | Ethanol | | | | | 497 | 0.07 | 515 | 0.08 |
| 3.4 | 2-Pentanone | 474 | 0.08 | 547 | 0.08 | 581 | 0.08 | 637 | 0.08 |
| 6.7 | Cyclopentanone | | | 1094 | 0.15 | 1884 | 0.23 | 2290 | 0.28 |
| 6.7 | 2-Methylcyclopentanone | | | 221 | 0.03 | 738 | 0.09 | 648 | 0.08 |
| 8.3 | 2-Hydroxy-3-butanone | 297 | 0.05 | 1272 | 0.19 | 12250 | 1.69 | 16267 | 2.21 |
| 8.6 | Hydroxyacetone | 609 | 0.17 | 1023 | 0.23 | 26579 | 5.64 | 34857 | 7.30 |
| 9.6 | 2-Methyl-2-cyclopenten-1-one | | | 5283 | 0.73 | 9626 | 1.23 | 9983 | 1.26 |
| 9.7 | 1-Hydroxy-2-butanone | | | | | 6999 | 1.07 | 10211 | 1.53 |
| 10.2 | 4-Hydroxy-3-hexanone | | | | | 973 | 0.13 | 1405 | 0.19 |

| | | | | | | | | | |
|---|---|---|---|---|---|---|---|---|---|
| 10.5 | 2-Pentyl-methoxyacetate | | | | | 2577 | 0.35 | 4141 | 0.56 |
| 10.6 | 4-Heptanol | | | | | 2822 | 0.33 | 4570 | 0.53 |
| 10.6 | 1-Hydroxy-2-pentanone | | | | | 1001 | 0.14 | 1533 | 0.21 |
| 10.8 | Acetic acid | 3120 | 0.86 | 6504 | 1.44 | 30588 | 6.32 | 19416 | 3.95 |
| 11.0 | Furfural | 7262 | 1.55 | 2977 | 0.51 | | | | |
| 11.5 | 2,5-Hexanedione | 1459 | 0.28 | 2898 | 0.44 | 4441 | 0.64 | 4209 | 0.59 |
| 11.9 | Propanoic acid | 1107 | 0.23 | 2927 | 0.49 | 17459 | 2.71 | 17713 | 2.72 |
| 12.5 | Propylene glycol | 226 | 0.05 | 610 | 0.10 | 4624 | 0.73 | 1002 | 0.16 |
| 13.0 | 1,2-Ethanediol | 598 | 0.14 | 1033 | 0.20 | 445 | 0.08 | 797 | 0.14 |
| 13.0 | Butanoic acid | | | 878 | 0.14 | | | | |
| 13.1 | γ-Butyrolactone | | | 340 | 0.05 | 774 | 0.10 | 2265 | 0.30 |
| 15.4 | 3-Methyl-1,2-cyclopentanedione | 995 | 0.18 | 2363 | 0.34 | | | 867 | 0.12 |
| 17.3 | Phenol | 411 | 0.06 | 1607 | 0.19 | 1673 | 0.18 | 2182 | 0.23 |
| 20.4 | 4-Oxopentanoic acid | 12670 | 2.79 | 1727 | 0.30 | 2029 | 0.33 | | |
| 21.8 | 5-Hydroxymethyl-2-furaldehyde | 298 | 0.06 | | | | | | |
| | Unknowns | | 2.85 | | 4.22 | | 7.75 | | 9.84 |
| | Light WS total | | 9.41 | | 9.91 | | 30.12 | | 32.61 |

[a]General reaction conditions: Glucose = 4 g, $H_2O$ = 40 g, atmosphere = 1.0 MPa ($N_2$), temperature = 300 °C, time = 10 min. Yields were calculated as carbon yield based on glucose. [b]$Fe_3O_4$ = 8.646 g. [c]Fe = 6.256 g. [d]Fe = 6.256 g, $Fe_3O_4$ = 8.646 g.

## 2. Hydrothermal reaction of benzaldehyde

Experimental procedure

Benzaldehyde (1 g, Wako Pure Chemical Industries, Ltd.), Fe powder (1.564 g, NM-0029-UP, Ionic Liquids Technologies GmbH), and deionized water (40 g) were introduced into the Hastelloy C high-pressure reactor (MMJ-100, OM Labotech), which was purged four times with nitrogen. The initial pressure was set to 1.0 MPa with nitrogen, and the stirring rate was adjusted to 700 rpm. The reactor was then heated to 300 ℃. After the reaction time elapsed, the reactor was rapidly cooled to 25 ℃ using ice-water. The filtered reaction mixture was diluted with acetone (1:1 v/v), and 2-methoxyethanol was added as an internal standard. Qualification and quantification of each product in the WS fraction was performed by GC-mass spectrometry on the Shimadzu QP-2010 system equipped with a capillary column (Inert-cap® WAX-HT, 30 m × 0.25 mm ID × 0.25 μm film thickness, GL Sciences), and GC-flame ionization detector on the Shimadzu GC-2014 equipped with same capillary column.

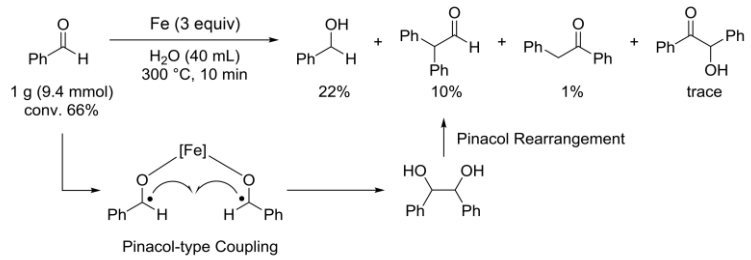


**Scheme S1.** Product yields and plausible mechanism of hydrothermal reaction of benzaldehyde.

### 3. Elemental balance of Fe-assisted hydrothermal liquefaction

The balance of elements in the starting material, products [WS, water-insoluble (WI), gas, and solid residue (SR)], and byproducts of hydrothermal liquefaction of oil palm empty fruit bunch (EFB) is summarized in Table S2. Elemental compositions were calculated using carbon yields and elemental ratios obtained in a previous study[1] (Table S3). The hydrogen generated from Fe was calculated assuming the reaction $3Fe + 4H_2O \rightarrow Fe_3O_4 + 4H_2$. Oxidation degrees of Fe were estimated using Rietveld X-ray diffraction (XRD) quantification of raw and spent iron powder (Table S4). The hydrogen and oxygen contents in SR could not be determined because of the interference of oxygen contained in oxidized Fe mixed in SR. $H_2O$ produced through dehydration of alcoholic products could not be quantified since the solvent was also $H_2O$. Therefore, it was impossible to completely balance the elements before and after the reaction. However, the total elemental compositions of the products, excluding those that cannot be calculated, do not largely diverge from those of the starting materials, indicating that the calculated values can be considered reasonable. On the basis of the calculations, the hydrogen expected to be generated from Fe is 182 mmol as H atom. We assume this amount is the reducing capacity of Fe. On the other hand, the $H_2$ in gas phase, quantified by GC-thermal conductivity detector after the reaction, is 93 mmol as H atom. Considering the difference between expected and generated $H_2$ in the gas phase, we estimate that, in the hydrothermal liquefaction reaction of EFB, about half of the reducing capacity of Fe was used for the reduction of the products, while the remaining half was used for the reaction with water to generate $H_2$.

**Table S2.** Elemental compositions of substrates and products of Fe-assisted hydrothermal liquefaction of EFB[a]

| | | Elemental composition (mmol) | | |
|---|---|---|---|---|
| | | C | H | O |
| Before Reaction | EFB | 148 | 188 | 114 |
| | Expected $H_2$ from Fe[b] | - | 182 | - |
| | total | 148 | 370 | 114 |
| Products | WS | 83 | 141 | 47 |
| | WI | 34 | 42 | 8 |
| | Gas | 6 | 1 | 10 |
| | SR | 15 | N/A | N/A |
| | total | 138 | 184 | 65 |
| $H_2$ in gas phase[c] | | - | 93 | - |
| $H_2O$ | | - | N/A | N/A |
| After Reaction total | | 138 | 277 | 65 |

[a]Reaction conditions: EFB = 4 g, $H_2O$ = 40 g, atmosphere = 1.0 MPa ($N_2$), temperature = 300 °C, time = 10 min. [b]$3Fe + 4H_2O \rightarrow Fe_3O_4 + 4H_2$. [c]Quantified by GC-TCD.

**Table S3.** Carbon yield and elemental ratio of each product from hydrothermal liquefaction of EFB[a]

| | Yield (%C) | H/C | O/C |
|---|---|---|---|
| WS | 56 | 1.70 | 0.57 |
| WI | 23 | 1.24 | 0.23 |
| Gas[b] | 4 | 0.21 | 1.68 |
| SR | 10 | N/A | N/A |
| total | 93 | | |

[a]Reaction conditions: EFB = 4 g, $H_2O$ = 40 g, atmosphere = 1.0 MPa ($N_2$), temperature = 300 °C, time = 10 min. Yields were calculated as carbon yield based on EFB. Data are from reference 1. [b]H/C and O/C ratios were calculated on the basis of GC analysis.

**Table S4.** Rietveld XRD quantification of raw and spent Fe powder[a]

| | Fe | $Fe_3O_4$ |
|---|---|---|
| Raw Fe | 70.6 | 29.4 |
| Spent Fe (SR of HTL) | 9.8 | 90.2 |

[a]XRD patterns were collected by the Rigaku SmartLab X-ray diffractometer using CuKα radiation at a voltage of 45 kV and current of 200 mA. Divergence slit = 1/3º, vertical divergence limitation = 13 mm, 2θ = 5–90º, step width = 0.02º, scanning speed = 5º $min^{-1}$. Diffraction data file on ICDD (International Centre for Diffraction Date) was employed. Reitveld analysis was conducted using the Rigaku-manufactured integrated X-ray powder diffraction software PDXL2 ver.2.7.3.

## 4. Hydrothermal liquefaction of lignin model substrates

Experimental procedure

The model substrate (1 g, as solid), Fe powder (1.564 g, Ionic Liquids Technologies GmbH, NM-0029-UP), and deionized water (40 g) were introduced into the Hastelloy C high-pressure reactor (MMJ-100, OM Labotech), which was purged four times with nitrogen. The initial pressure was set to 1.0 MPa with nitrogen, and the stirring rate was adjusted to 700 rpm. The reactor was then heated to 300 °C. After the reaction time elapsed, the reactor was rapidly cooled to 25 °C using ice-water. Products were separated into WS, WI, gas, and SR fractions, and yields were determined according to the method described in the text.

**Table S5.** Hydrothermal liquefaction of model substrates bearing various lignin contents[a]

| Substrate | Lignin content (%) | Fe (g) | Yields (%C) | | | | Carbon Balance (%C) |
|---|---|---|---|---|---|---|---|
| | | | WS | WI | Gas | SR | |
| (A) Cellulose/Xylan (6:4) | 0 | 1.564 | 94 | 1 | 2 | 4 | 101 |
| (A) Cellulose/Xylan (6:4) | 0 | 0 | 60 | 22 | 5 | 6 | 94 |
| (B) EFB | 27 | 1.564 | 69 | 15 | 5 | 8 | 97 |
| (B) EFB | 27 | 0 | 51 | 31 | 6 | 6 | 94 |
| (C) Enzymatic lignin | 61 | 1.564 | 43 | 35 | 4 | 11 | 93 |
| (C) Enzymatic lignin | 61 | 0 | 34 | 40 | 5 | 13 | 93 |
| (D) Alkali lignin | 100 | 1.564 | 18 | 65 | 1 | 17 | 103 |
| (D) Alkali lignin | 100 | 0 | 14 | 56 | 1 | 31 | 102 |

[a]Reaction conditions: Substrates = 1 g (as solid), $H_2O$ = 40 g, atmosphere = 1.0 MPa ($N_2$), temperature = 300 °C, time = 10 min. Yields were calculated as carbon yield based on the starting materials.

## 5. Reference

(1) Miyata, Y.; Yamazaki, Y.; Hirano, Y.; Kita, Y. Quantitative Analysis of the Aqueous Fraction from the Fe-Assisted Hydrothermal Liquefaction of Oil Palm Empty Fruit Bunches. *J. Anal. Appl. Pyrolysis* **2018**, *132*, 72–81.